J. Fluid Mech. (1995), *vol.* 297, *pp.* 327–355

Analytical solutions for the actuator disk with variable radial distribution of load

By JOHN T. CONWAY

Agder College, Grimstad, Norway

(Received 17 March 1994 and in revised form 23 March 1995)

An analytical method somewhat analogous to finite wing theory has been developed which enables the flow induced by a linearized propeller actuator disk with variable radial distribution of load to be solved in closed form for the first time. Analytical solutions are given for various load distributions including the case of an arbitrary polynomial loading. As in finite wing theory, the case of elliptic loading is exceptionally simple and the induced velocities and stream function are simple expressions of elementary functions. Results are also given for a practical propeller load distribution with finite hub. The method can also be used to solve a wide range of analogous electromagnetic problems.

1. Introduction

The problem of calculating the velocity fields induced by an actuator disk is of technological interest to both the aeronautical and hydronautical industries. Because of the obvious difficulties of performing unsteady calculations on the continuously changing geometry resulting from the relative rotation of a propeller and its vehicle, an actuator disk approach is sometimes employed even in sophisticated Navier–Stokes calculations such as those of Stern *et al.* (1988). In the aerospace industry, the propeller influence on the aircraft is routinely calculated using boundary integral (panel) methods incorporating some kind of actuator disk. To model compressibility effects these methods employ a wide range of compressibility corrections of Göthert–Prandtl–Glauert type, and the theory presented here can also be extended into the high subsonic regime in this manner. For hydronautical applications, flow velocities are always so small a fraction of the very high speed of sound in water (1531 m s^{-1}) that compressibility effects are negligible. A typical method of this type is a version of the VSAERO computer code by Strash *et al.* (1984), which represents the actuator disk as discrete panels, and the slipstream for a variable radial distribution of load as concentric cylinders of panels. This approach has a number of practical disadvantages, and cannot really be considered a fully satisfactory solution to the problem. A more satisfactory brute-force method is that of Clark & Valarezo (1990), which solves using a panel method for the isolated propeller flow in the blade-fixed coordinate system to obtain a time-averaged perturbation to the free stream for an additional panel calculation in the vehicle-fixed coordinate system. This method can predict propeller–vehicle interactions satisfactorily but has the disadvantage that a complete detailed panel model of the propeller must be available. Hence it cannot be used in initial design to explore the effect of different blade loadings on the vehicle. An analytical solution for arbitrary radial loading could be incorporated into boundary

integral methods to combine all the advantages of the above methods together with greater simplicity. It is the purpose of this article to present such a solution derived using the methods of classical analysis.

The analytical solution for the velocity fields induced by an actuator disk with constant radial distribution of load has been given by Hough & Ordway (1965), who also constructed by superposition the solution for general radial distributions of load as integrals of the constant-loading solutions. However, these integrals appeared sufficiently complex to discourage anything other than numerical integration. The method presented here is based on construction of the velocity and potential fields induced by a ring vortex as integrals over the allowed values of the separation constant of the eigensolutions of Laplace's equation in cylindrical coordinates. The ring vortex solutions are then combined to give the solutions for the constant-load and general actuator disks as double and triple integrals respectively of the eigensolutions. The axial integrations can be performed immediately, and the solution for the constant-loaded disk is then completed by integrating over the values of the separation constant.

If, for the general actuator disk, the integral over the values of the separation constant is performed before the radial integration, then equations closely related to those of Hough & Ordway (1965) and an additional equation for the vector potential are obtained. It has been found that by representing the radial variation of axial velocity at the actuator disk as an arbitrary polynomial, an additional integration of these equations can be performed which reduces the solutions to integrals of elementary functions.

If the radial integrations in the general integrals are performed first, an entirely new method is obtained which gives completely analytic solutions in terms of elliptic integrals for the velocities and vector potential by representing the radial variation of load as an even polynomial. For the special case of an elliptic radial distribution of load, analytic solutions for the velocities and vector potential can also be obtained by this method which are simple expressions involving only elementary functions.

In §2 below, the representation of the fields of a ring vortex in terms of eigensolutions of Laplace's equation is derived, and these are then integrated to give the usual expressions in terms of elliptic integrals for the velocity components and vector potential, together with an additional elliptic integral expression for the scalar potential, which is believed to be new. In §3 the equations for the constant-loaded actuator disk are derived, which are then integrated to give the expressions obtained by Hough & Ordway (1965) for the velocity fields and new expressions for the vector and scalar potentials. Section 4 gives the derivation of the solutions for the generalized actuator disk in terms of eigenfunction integrals and also discusses optimum load distributions within the context of actuator disk theory. In §5 the methods of solution developed for the actuator disk equations are described. Explicit formulae and results are given for parabolic and elliptic radial distributions of load, and results are presented for a practical propeller load distribution with a finite hub. Simplified formulae for the axis of symmetry are also given. Table 1 lists the special functions used.

2. The velocity and potential fields induced by a ring vortex

The starting point for the development of the current method is the fields induced by a ring vortex. From the Biot-Savart law the velocity $\mathrm{d}\boldsymbol{V}$ induced at position $\boldsymbol{r}$ by

Symbol	Special function
$E(\beta,k)$	Elliptic integral of the second kind
$\mathrm{E}(k)$	Complete elliptic integral of the second kind
$F(\beta,k)$	Elliptic integral of the first kind
$J_v(x)$	Bessel function of the first kind
$\mathrm{K}(k)$	Complete elliptic integral of the first kind
$Q_v(x)$	Legendre function of the second kind
$Q_v^\mu(x)$	Associated Legendre function of the second kind
$\Gamma(x)$	Gamma function
$\delta(x)$	Dirac delta function
$H(x)$	Heaviside step function
$\Lambda_0(\beta,k)$	Heuman's Lambda function

TABLE 1. Special functions used

a vortex element $\Gamma \mathrm{d}\boldsymbol{l}'$ placed at position $\boldsymbol{r}'$ is given by

$$\mathrm{d}\boldsymbol{V}(\boldsymbol{r}) = \frac{\Gamma \mathrm{d}\boldsymbol{l}' \times (\boldsymbol{r} - \boldsymbol{r}')}{4\pi |\boldsymbol{r} - \boldsymbol{r}'|^3}. \tag{2.1}$$

The velocity field of a ring vortex can be constructed as the superposition of the velocities induced by each vortex line element making up the vortex. In cylindrical polar coordinates (r, ϕ, z), a vortex ring of radius a placed at $z = z'$ has by symmetry a zero azimuthal velocity component $V_\phi(r,z)$ and the other two velocity components are given by the integrals below:

$$V_r(r,z) = \frac{\Gamma a}{4\pi} \int_0^{2\pi} \frac{(z-z')\cos\phi' \mathrm{d}\phi'}{\{a^2 + r^2 - 2ar\cos\phi' + (z-z')^2\}^{3/2}}, \tag{2.2}$$

$$V_z(r,z) = \frac{\Gamma a}{4\pi} \int_0^{2\pi} \frac{(a - r\cos\phi')\mathrm{d}\phi'}{\{a^2 + r^2 - 2ar\cos\phi' + (z-z')^2\}^{3/2}}. \tag{2.3}$$

Solutions can be stated for these integrals in terms of complete elliptic integrals, but these are relatively intractable for constructing the flow within a slipstream as either a surface or volume distribution of ring vortices. However, for field points along the axis of symmetry then $V_r(0,z) = 0$, and (2.3) can be integrated to give the simple result

$$V_z(0,z) = \frac{\Gamma a^2}{2(a^2 + (z-z')^2)^{3/2}}. \tag{2.4}$$

The velocity field $\boldsymbol{V}$ induced by a ring vortex can also be obtained from either the velocity potential Φ through $\boldsymbol{V} = \nabla\Phi$, or from the vector (solenoidal) potential $\boldsymbol{A}$ through $\boldsymbol{V} = \nabla \times \boldsymbol{A}$. For axisymmetric flows A_ϕ is the only non-zero component of $\boldsymbol{A}$ and $\psi = rA_\phi$, where ψ is the axial stream function.

For incompressible inviscid flow Φ, $\boldsymbol{A}$ and the velocity $\boldsymbol{V}$ all satisfy Laplace's equation. Hence for a ring vortex centred on the origin normal to the z-axis, the $V_z(r,z)$ field induced by the vortex is a superposition of the allowable solutions of Laplace's equation obtained by separating the variables. The only elementary solution finite on the z-axis and which $\to 0$ as $|z - z'| \to \infty$ is

$$V(r,z) = A_s \mathrm{e}^{-s|z-z'|} J_0(sr). \tag{2.5}$$

All positive values of s are allowable, so the V_z field induced by the ring vortex is of the form

$$V_z(r,z) = \int_0^\infty A(s)\mathrm{e}^{-s|z-z'|}J_0(sr)\mathrm{d}s. \tag{2.6}$$

On the axis of symmetry, $V_z(0,z)$ must reduce to (2.4) and from (2.6), it is also given by the Laplace transform of $A(s)$. Hence inverting the Laplace transform to solve for $A(s)$ (Spiegel 1965) gives the alternative integral representation below for $V_z(r,z)$:

$$V_z(r,z) = \frac{\Gamma a}{2}\int_0^\infty sJ_1(sa)J_0(sr)\mathrm{e}^{-s|z-z'|}\mathrm{d}s. \tag{2.7}$$

The other fields corresponding to (2.7) are clearly

$$V_r(r,z) = \frac{\pm\Gamma a}{2}\int_0^\infty sJ_1(sa)J_1(sr)\mathrm{e}^{-s|z-z'|}\mathrm{d}s, \tag{2.8}$$

$$\Phi(r,z) = \frac{\mp\Gamma a}{2}\int_0^\infty J_1(sa)J_0(sr)\mathrm{e}^{-s|z-z'|}\mathrm{d}s, \tag{2.9}$$

$$A_\phi(r,z) = \frac{\Gamma a}{2}\int_0^\infty J_1(sa)J_1(sr)\mathrm{e}^{-s|z-z'|}\mathrm{d}s. \tag{2.10}$$

In (2.8) above, the positive sign is to be taken for $(z-z') > 0$ and the negative sign for $(z-z') < 0$. The reverse is true for (2.9). This does not give rise to a discontinuous radial field as $V_r(r,z) = 0$ for $(z-z') = 0$. However, the scalar potential changes by $-\Gamma$ at the plane of the ring vortex when passing through the ring in the direction of positive z.

Equations (2.7) to (2.10) above can be obtained in a number of other ways and lie at the core of the current work. They have been known since the early days of fluid mechanics and are given by Basset (1888) and Lamb (1932), but later general texts have tended to omit them. Wu (1962) has applied these formulae to the heavily loaded actuator disk.

Equation (2.10) can be integrated (Gradshteyn & Ryzhik 1980) to give

$$A_\phi(r,z) = \frac{\Gamma}{2\pi}\left(\frac{a}{r}\right)^{1/2}Q_{1/2}(\omega_1) \tag{2.11}$$

where

$$\omega_1 \equiv 1 + \frac{(a-r)^2 + (z-z')^2}{2ar}. \tag{2.12}$$

This corresponds to the axisymmetric stream function

$$\psi(r,z) = \frac{\Gamma(ar)^{1/2}}{2\pi}Q_{1/2}(\omega_1). \tag{2.13}$$

Equation (2.13) is a central element of the approaches of Hough & Ordway (1965) and Greenberg & Powers (1970). It is the Green's function for the stream function induced by a distribution of ring vortices.

The Legendre function above is singular for unit argument, corresponding to the infinite velocities induced by a vortex ring as the ring itself is approached. This means that approaches using (2.13) as the starting point necessarily involve singular integrals. A recurrent theme of the current work is to side-step (2.13) and instead use (2.7) to (2.10) directly to construct the flow induced by distributions of ring vortices. The advantage of this is that for the eigensolutions resulting from separation of variables,

the variables are indeed separated, which permits repeated integration within multi-dimensional integrals to be performed analytically and in the most convenient order. Equations (2.7) to (2.9) can also be integrated to give closed-form solutions for the other fields. If we define

$$k_1 \equiv \left(\frac{4ar}{(a+r)^2 + (z-z')^2} \right)^{1/2} \tag{2.14}$$

then the velocity fields are given by (Prudnikov, Brychkov & Marichev 1992):

$$V_r(r,z) = \frac{\Gamma(z-z')k_1 \left[(2-k_1^2)\mathrm{E}(k_1) - 2(1-k_1^2)\mathrm{K}(k_1)\right]}{8\pi(1-k_1^2)(ar^3)^{1/2}}, \tag{2.15}$$

$$V_z(r,z) = \frac{\Gamma k_1 \left[k_1^2(a^2-r^2-z^2)\mathrm{E}(k_1) + 4ra(1-k_1^2)\mathrm{K}(k_1)\right]}{16\pi(1-k_1^2)(ra)^{3/2}}. \tag{2.16}$$

These results can of course also be obtained directly from (2.2) and (2.3). The scalar potential of the ring vortex can be obtained by integrating (2.9) (Prudnikov *et al.* 1992, but note the typographical errors). Let

$$\beta_1 \equiv \arcsin\left\{ \frac{z-z'}{((z-z')^2 + (r-a)^2)^{1/2}} \right\} \tag{2.17}$$

where the function $\arcsin(x)$ is defined everywhere in this article on the interval $(-\pi/2, \pi/2)$. Then

$$\Phi(r,z) = \frac{\Gamma}{4}\left\{ \frac{(z-z')k_1\mathrm{K}(k_1)}{\pi(ar)^{1/2}} + \Lambda_0(\beta_1,k_1) \mp 2 \right\} \quad (r < a) \tag{2.18}$$

and

$$\Phi(r,z) = \frac{\Gamma}{4}\left\{ \frac{(z-z')k_1\mathrm{K}(k_1)}{\pi(ar)^{1/2}} - \Lambda_0(\beta_1,k_1) \right\} \quad (r > a). \tag{2.19}$$

The Bessel–Laplace integral of (2.9) is not well known and infrequently tabulated. The Heuman Lambda function Λ_0 which appears in (2.18) and (2.19) forms a key element in the solutions derived by Hough & Ordway (1965) for the uniformly loaded actuator disk, and it also occurs in most of the additional solutions presented here. It is tabulated by Abramowitz & Stegun (1972) and is defined in terms of elliptic integrals of the first and second kinds. If k' is the complementary modulus for an elliptic integral of modulus k, then

$$\Lambda_0(\beta,k) \equiv \frac{2}{\pi}\left[\mathrm{E}(k)F(\beta,k') + \mathrm{K}(k)E(\beta,k') - \mathrm{K}(k)F(\beta,k')\right] \tag{2.20}$$

(Prudnikov *et al.* 1992; Abramowitz & Stegun 1972). The solution given by (2.18) and (2.19) for the scalar potential of a ring vortex is more useful computationally than the usual solid angle formula and is believed to be new.

3. Actuator disk with uniform axial inflow

For an unsteady incompressible flow the instantaneous velocity fields are linearly related to the instantaneous vorticity distribution via the Biot-Savart law. Hence the time-averaged velocity fields are given by the steady flow induced by the time-average of the vorticity distribution. If the bound circulation of the blades of a

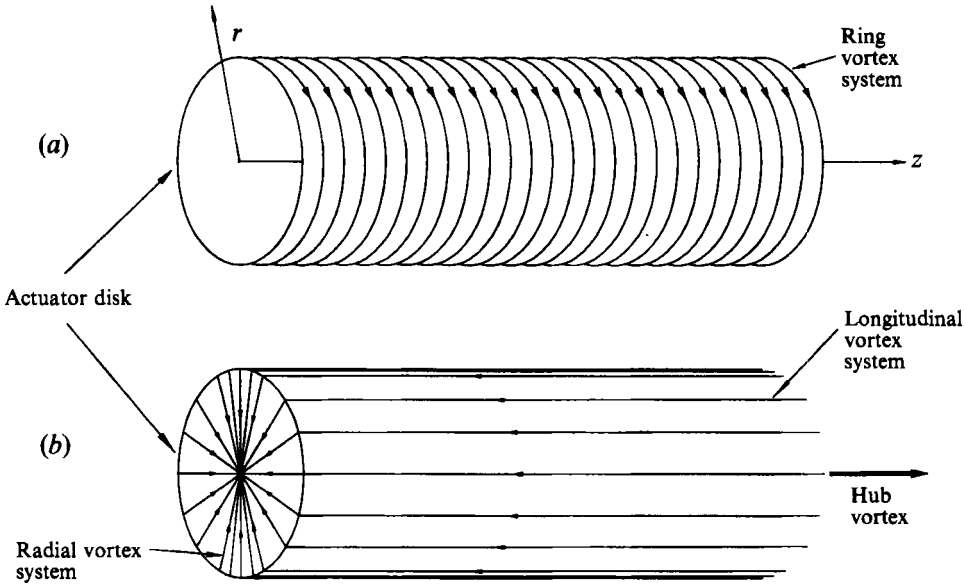

FIGURE 1. Self-conserving vortex systems of the uniformly loaded actuator disk. The slipstream contraction is not shown. (*a*) Vortex system 1, which induces the axial and radial velocities. (*b*) Vortex system 2, which induces the azimuthal velocity.

propeller is represented by straight lifting lines which lie in a plane, then the time-averaged velocity field induced by the propeller is correctly given by the actuator disk model. The instantaneous pressure field is nonlinearly related to the vorticity via the Bernoulli equation, so the thrust and torque on the propeller are only given to the approximation to which the Bernoulli equation can be linearized for small perturbations or in the limit of infinite blade number when the flow becomes steady. Hence the thrust and torque of a propeller are blade-number dependent, as is the optimum distribution of circulation along the blades.

The actuator disk with uniform axial inflow has been intensively studied and has been used as the basic building block for general methods which construct the general actuator disk solution by superposition. The time-average of the bound and shed vorticity of the propeller is the superposition of the vorticity distributions shown in figure 1. There are four vortex distributions which induce perturbations to the free-stream flow. These are:

(i) a vortex tube consisting of ring vortices distributed over a contracting tube shed from the edge of the actuator disk and extending to downstream infinity;

(ii) the constant-strength hub vortex along the axis of symmetry of the disk and extending from the disk centre to downstream infinity;

(iii) a distribution of radial vorticity on the actuator disk;

(iv) a surface distribution of vorticity on the slipstream surface normal to the ring vortices and equal in strength to the hub vortex.

Superposition of these distributions results in helical vortex lines in the slipstream surface. Distribution (i) forms a vorticity-conserving system and distributions (ii), (iii) and (iv) together also form a vorticity-conserving system. Hence these two systems can be superimposed in any relative proportion while still conserving vorticity. Distribution (iii) results from the lifting lines of the propeller blades and distributions (i), (ii) and (iv) result from the the root and tip vortices shed from these lifting lines.

Distribution (ii) gives an infinite force on the actuator disk, and therefore this simple model cannot be used directly to estimate propeller efficiencies. For the case of a contra-rotating propeller or a single-rotating propeller when rotation in the propeller wake can be neglected, then only distribution (i) is considered and crude estimates of propeller efficiency can then be obtained from elementary actuator disk theory. The power P supplied to a propeller with frequency of rotation n is related to the torque Q through the relation $P = 2\pi nQ$. Hence the torque can be estimated indirectly from the efficiency η, the thrust coefficient τ and the power coefficient σ from the identity below (Von Mises 1945)

$$\eta \equiv \frac{\tau}{\sigma}, \text{ where } \sigma \equiv \frac{2P}{\pi\rho U_\infty^3 R_a^2} \text{ and } \tau \equiv \frac{2T}{\pi\rho U_\infty^2 R_a^2}. \tag{3.1}$$

For the linearized actuator disk, the two vorticity-conserving systems above are essentially independent and their induced velocity fields can be solved separately.

3.1. *Longitudinal vortex system*

This consists of the vortex distributions (ii), (iii) and (iv) above. By using the axial symmetry of the distributions together with Stoke's theorem, it is simple to show that regardless of axial position or the contraction of the slipstream, V_ϕ is the only non-zero velocity component, and is given by

$$V_\phi(r,z) = \frac{\Gamma_{hub}}{2\pi r} \quad (r < R(z) \text{ and } z > 0), \tag{3.2}$$

$$V_\phi(r,z) = 0 \quad (r > R(z) \text{ or } z < 0). \tag{3.3}$$

Hence this velocity field does not influence the slipstream contraction directly. The velocity induced by distributions (ii) and (iv) on the lifting-line distribution (iii) is clearly one half of that given by (3.2).

3.2. *Ring vortex system*

This vortex system is directly responsible for the slipstream contraction and all axial and radial velocities. Using the integral representation in terms of Bessel functions developed earlier, and introducing an axial distribution function $\gamma(z)$ for the ring vortices, then we obtain

$$V_r(r,z) = \frac{1}{2}\int_0^\infty \int_0^\infty \pm\gamma(z')sR(z')J_1(sR(z'))J_1(sr)e^{-s|z-z'|}ds\,dz', \tag{3.4}$$

$$V_z(r,z) = \frac{1}{2}\int_0^\infty \int_0^\infty \gamma(z')sR(z')J_1(sR(z'))J_0(sr)e^{-s|z-z'|}ds\,dz', \tag{3.5}$$

$$A_\phi(r,z) = \frac{1}{2}\int_0^\infty \int_0^\infty \gamma(z')R(z')J_1(sR(z'))J_1(sr)e^{-s|z-z'|}ds\,dz'. \tag{3.6}$$

In these expressions $R(z)$ is the slipstream radius at axial coordinate z and $\gamma(z)$ is the vortex density per unit axial coordinate. Equations (3.4) to (3.6) are extremely tractable because we can choose the order of integration as necessary. For example, if we set $r = 0$ in (3.5) and integrate first with respect to s (Gradshteyn & Ryzhik 1980) we obtain

$$V_z(0,z) = \frac{1}{2}\int_0^\infty \frac{\gamma(z')R^2(z')dz'}{(R^2(z') + (z-z')^2)^{3/2}}. \tag{3.7}$$

This result can of course be obtained by more elementary means.

Infinitely far downstream then clearly $\gamma(z \to \infty) = U_d$, the constant axial perturbation velocity everywhere within the slipstream at downstream infinity. For the linearized actuator disk, the convection velocity of the ring vortices is approximated by the free-stream velocity U_∞ and therefore $\gamma(z)$ is constant and equal to U_d. We can also approximate $R(z)$ by R_a, the radius of the actuator disk. With these approximations, (3.7) can be integrated again to give

$$V_z(0,z) = \frac{U_d}{2}\left\{1 + \frac{z}{(R_a^2 + z^2)^{1/2}}\right\}. \tag{3.8}$$

This axial velocity distribution is derived by Koning (1935) using somewhat different assumptions than those made here.

Putting $z = 0$ in (3.8) gives $V_z(r,0) = U_d/2$ for $r < R_a$, in agreement with elementary actuator disk theory, and hence applying the Bernoulli equation on both sides of the disk with $V_\phi = 0$ gives the thrust coefficient as

$$\tau = \frac{U_d}{U_\infty}\left(2 + \frac{U_d}{U\infty}\right), \tag{3.9}$$

as in the elementary theory.

Substituting $R(z') = R_a$, and $\gamma(z') = U_d$ in (3.4) to (3.6) and integrating with respect to z' gives

$$V_r(r,z) = \frac{-U_d R_a}{2}\int_0^\infty \mathrm{e}^{-s|z|} J_1(sR_a)J_1(sr)\mathrm{d}s, \tag{3.10}$$

$$V_z(r,z) = \frac{U_d R_a}{2}\int_0^\infty (2 - \mathrm{e}^{-s|z|})J_1(sR_a)J_0(sr)\mathrm{d}s \quad (z \geqslant 0), \tag{3.11}$$

$$V_z(r,z) = \frac{U_d R_a}{2}\int_0^\infty \mathrm{e}^{-s|z|} J_1(sR_a)J_0(sr)\mathrm{d}s \quad (z < 0), \tag{3.12}$$

$$A_\phi(r,z) = \frac{U_d R_a}{2}\int_0^\infty \left(\frac{2 - \mathrm{e}^{-s|z|}}{s}\right) J_1(sR_a)J_1(sr)\mathrm{d}s \quad (z \geqslant 0), \tag{3.13}$$

$$A_\phi(r,z) = \frac{U_d R_a}{2}\int_0^\infty \frac{J_1(sR_a)J_1(sr)\mathrm{e}^{-s|z|}}{s}\mathrm{d}s \quad (z < 0). \tag{3.14}$$

For the uniformly loaded actuator disk, it is also possible to define a scalar potential $\Phi(r,z)$. From inspection of (3.10) to (3.14) this is given by

$$\Phi(r,z) = \frac{U_d}{2}(z + |\,z\,|) + \frac{U_d R_a}{2}\int_0^\infty \frac{J_1(sR_a)J_0(sr)}{s}\mathrm{e}^{-s|z|}\mathrm{d}s. \tag{3.15}$$

Using the integral tables of Gradshteyn & Ryzhik (1980) and Prudnikov *et al.* (1992), (3.10) to (3.15) can be integrated again with respect to s to give the complete solution for fields induced by a linearized actuator disk with constant radial loading. The results are

$$V_r(r,z) = \frac{-U_d}{2\pi}\left(\frac{R_a}{r}\right)^{1/2} Q_{1/2}(\omega), \tag{3.16}$$

$$V_z(r,z) = \frac{U_d}{4}\left\{\frac{z}{\pi(R_a r)^{1/2}}Q_{-1/2}(\omega) + \Lambda_0(\beta,k) + 2\right\} \quad (r < R_a), \tag{3.17}$$

$$V_z(r,z) = \frac{U_d}{4}\left\{\frac{z}{\pi(R_a r)^{1/2}}Q_{-1/2}(\omega) - \Lambda_0(\beta,k)\right\} \quad (r > R_a), \tag{3.18}$$

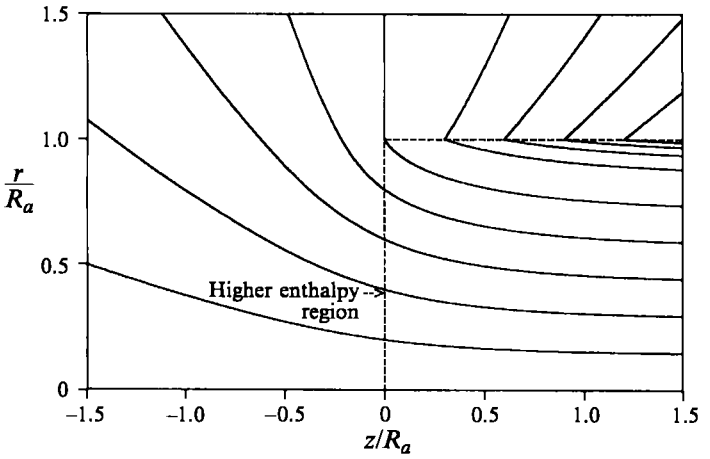

FIGURE 2. Perturbation streamline pattern for the uniformly loaded actuator disk. The broken line encloses the higher enthalpy region of the flow.

$$A_\phi(r,z) = \frac{U_d z}{2\pi}\left\{\frac{-\mathrm{E}(k)}{k}\left(\frac{R_a}{r}\right)^{1/2} + \frac{k(z^2+2R_a^2+2r^2)\mathrm{K}(k)}{4\left(R_a r^3\right)^{1/2}}\right\} + \frac{U_d}{4}\left\{\frac{-\mid R_a^2-r^2\mid \Lambda_0(\beta,k)}{2r} + r\right\} \quad (r<R_a), \tag{3.19}$$

$$A_\phi(r,z) = \frac{U_d z}{2\pi}\left\{\frac{-\mathrm{E}(k)}{k}\left(\frac{R_a}{r}\right)^{1/2} + \frac{k(z^2+2R_a^2+2r^2)\mathrm{K}(k)}{4\left(R_a r^3\right)^{1/2}}\right\} + \frac{U_d}{4}\left\{\frac{-\mid R_a^2-r^2\mid \Lambda_0(\beta,k)}{2r} + \frac{R_a^2}{r}\right\} \quad (r\geqslant R_a), \tag{3.20}$$

$$\Phi(r,z) = U_d\left\{\frac{z}{2} + \frac{(rR_a)^{1/2}}{\pi k}\mathrm{E}(k) + \frac{k(R_a^2-r^2)}{4\pi(rR_a)^{1/2}}\mathrm{K}(k) + \frac{z}{4}\Lambda_0(\beta,k)\right\} \quad (r<R_a), \tag{3.21}$$

$$\Phi(r,z) = U_d\left\{\frac{z+\mid z\mid}{2} + \frac{(rR_a)^{1/2}}{\pi k}\mathrm{E}(k) + \frac{k(R_a^2-r^2)}{4\pi\,(rR_a)^{1/2}}\mathrm{K}(k) - \frac{z}{4}\Lambda_0(\beta,k)\right\} \quad (r>R_a), \tag{3.22}$$

where

$$k \equiv \left(\frac{4R_a r}{(R_a+r)^2+z^2}\right)^{1/2},\quad \beta \equiv \arcsin\left\{\frac{z}{\left[z^2+(R_a-r)^2\right]^{1/2}}\right\} \text{ and } \omega \equiv \frac{z^2+r^2+R_a^2}{2rR_a}.$$

Equations (3.16) to (3.18) are the solutions given by Hough & Ordway (1965) for the velocity fields induced by a uniformly loaded actuator disk, which they derived by a quite different method from the above. They did not give analytical solutions for the vector and scalar potentials and (3.19) to (3.22) are believed to be new.

The axial stream function is given by $\psi(r,z) = rA_\phi(r,z)$ and the perturbation flow streamline pattern derived from (3.19) and (3.20) is plotted in figure 2. The

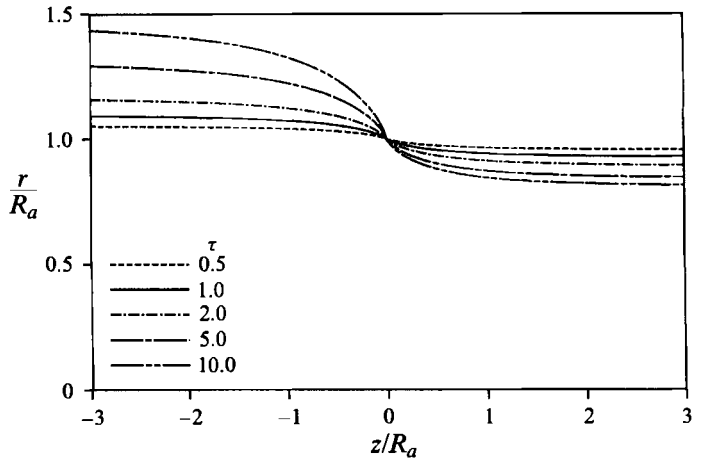

FIGURE 3. Slipstream contractions for the uniformly loaded actuator disk for different thrust coefficients. The curves show the streamlines which pass through the rim of the disk.

perturbation streamlines correspond to the limiting case as the thrust coefficient τ tends to infinity, which is equivalent to the case of a propeller rotating in still air. The linearized theory presented here is of course more accurate the smaller the value of τ. If the perturbation stream function is combined with that for a uniform free stream, then the slipstream contraction can be calculated. Figure 3 gives the predicted slipstream contractions for various values of the thrust coefficient τ.

Equations (3.21) and (3.22) could be used to construct by superposition an actuator disk model with variable radial loading suitable for implementation in a potential-based panel method. In the next section a much better general method is derived, which allows analytic solutions to be obtained for essentially arbitrary radial loading. This method is however best suited for implementation in a velocity-based panel method where a velocity potential need not be defined.

4. Actuator disk with arbitrary radial loading

4.1. *General formulae for fields induced by the ring vortex system*

In the linear limit where radial contraction is not considered, the case of arbitrary radial loading is obtained as a superposition of a radial distribution of vortex tubes, with each vortex tube having constant radius and surface ring vortex density. With $\gamma(r)$ redefined as the strength of the vortex tubes, superposition of elementary solutions such as (3.10) to (3.14) gives

$$V_r(r,z) = -\frac{1}{2}\int_0^{R_a}\int_0^{\infty} \gamma(r')\mathrm{e}^{-s|z|}r'J_1(sr')J_1(sr)\mathrm{d}s\,\mathrm{d}r', \tag{4.1}$$

$$V_z(r,z) = \frac{1}{2}\int_0^{R_a}\int_0^{\infty} \gamma(r')(2-\mathrm{e}^{-s|z|})r'J_1(sr')J_0(sr)\mathrm{d}s\,\mathrm{d}r' \quad (z \geqslant 0), \tag{4.2}$$

$$V_z(r,z) = \frac{1}{2}\int_0^{R_a}\int_0^{\infty} \gamma(r')\mathrm{e}^{-s|z|}r'J_1(sr')J_0(sr)\mathrm{d}s\,\mathrm{d}r' \quad (z < 0), \tag{4.3}$$

$$A_\phi(r,z) = \frac{1}{2}\int_0^{R_a}\int_0^{\infty} \gamma(r')\left(\frac{2-\mathrm{e}^{-s|z|}}{s}\right) r' J_1(sr')J_1(sr)\mathrm{d}s\,\mathrm{d}r' \quad (z \geqslant 0), \tag{4.4}$$

$$A_\phi(r,z) = \frac{1}{2}\int_0^{R_a}\int_0^{\infty} \gamma(r')\frac{\mathrm{e}^{-s|z|}}{s} r' J_1(sr')J_1(sr)\mathrm{d}s\,\mathrm{d}r' \quad (z < 0). \tag{4.5}$$

For $z = 0$, (4.2) and (4.3) above both give

$$V_z(r,0) = \frac{1}{2}\int_0^{R_a}\int_0^{\infty} \gamma(r') r' J_1(sr')J_0(sr)\mathrm{d}s\,\mathrm{d}r'. \tag{4.6}$$

Since $\gamma(r)$ is zero for $r > R_a$, the limit of the radial integration of (4.6) can be replaced by ∞ to give the first-order Hankel transform of γ, $\hat{\gamma}(s)$. Therefore

$$V_z(r,0) = \frac{1}{2}\int_0^{\infty} \hat{\gamma}(s)J_0(sr)\mathrm{d}s. \tag{4.7}$$

Taking the derivative of both sides of this equation with respect to r inverts the Hankel transform to give

$$\frac{\mathrm{d}V_z(r,0)}{\mathrm{d}r} = \frac{-\gamma(r)}{2}. \tag{4.8}$$

Equation (4.8) is a key element of the method presented here. It determines $\gamma(r)$ from a prescribed axial velocity distribution at the actuator disk. Using this equation, the velocities and vector potential induced by an actuator disk with arbitrary prescribed axial inflow can be written as

$$V_r(r,z) = \int_0^{\infty}\int_0^{\infty} \frac{\mathrm{d}V_z(r',0)}{\mathrm{d}r'}\mathrm{e}^{-s|z|} r' J_1(sr')J_1(sr)\mathrm{d}s\,\mathrm{d}r', \tag{4.9}$$

$$V_z(r,z) = -\int_0^{\infty}\int_0^{\infty} \frac{\mathrm{d}V_z(r',0)}{\mathrm{d}r'}(2-\mathrm{e}^{-s|z|}) r' J_1(sr')J_0(sr)\mathrm{d}s\,\mathrm{d}r' \quad (z \geqslant 0), \tag{4.10}$$

$$V_z(r,z) = -\int_0^{\infty}\int_0^{\infty} \frac{\mathrm{d}V_z(r',0)}{\mathrm{d}r'}\mathrm{e}^{-s|z|} r' J_1(sr')J_0(sr)\mathrm{d}s\,\mathrm{d}r' \quad (z < 0), \tag{4.11}$$

$$A_\phi(r,z) = -\int_0^{\infty}\int_0^{\infty} \frac{\mathrm{d}V_z(r',0)}{\mathrm{d}r'}\left(\frac{2-\mathrm{e}^{-s|z|}}{s}\right) r' J_1(sr')J_1(sr)\mathrm{d}s\,\mathrm{d}r' \quad (z \geqslant 0), \tag{4.12}$$

$$A_\phi(r,z) = -\int_0^{\infty}\int_0^{\infty} \frac{\mathrm{d}V_z(r',0)}{\mathrm{d}r'}\frac{\mathrm{e}^{-s|z|}}{s} r' J_1(sr')J_1(sr)\mathrm{d}s\,\mathrm{d}r' \quad (z < 0). \tag{4.13}$$

For any radial distribution of axial velocity which goes to zero continuously at the actuator disk rim, the upper limit of the radial integration can be conveniently replaced with R_a. However, for distributions which fall discontinuously to zero at the rim, such as a uniform distribution, the limit of integration must be taken as $R_a + \epsilon$, where ϵ is an infinitesimal positive quantity. This ensures that the delta-function component of the derivative of $V_z(r',0)$ is completely captured by the range of integration. An immediate consequence of (4.10) is that for arbitrary axial velocity distribution, as in elementary momentum theory,

$$V_z(r,0) = \frac{V_z(r,\infty)}{2}. \tag{4.14}$$

Equation (4.9) gives immediately the result that $V_r(r,z)$ is an even function of z, and hence continuous across the actuator disk.

For an arbitrary distribution of tube vortices, each tube vortex is also a surface of constant enthalpy on which Bernoulli's equation holds. Applying the Bernoulli equation on each side of the actuator disk in the same manner as for elementary momentum disk theory, making use of (4.14) , the continuity of V_r across the disk, together with the condition of continuity of pressure and mechanical equilibrium far downstream, it is straightforward to show that the pressure discontinuity across the actuator disk is related to the axial and azimuthal velocities by

$$\Delta P(r) = 2\rho(U_\infty + V_z(r,0))V_z(r,0) - \frac{\rho V_\phi^2(r,\infty)}{2}. \tag{4.15}$$

In the linear limit, this becomes

$$\Delta P(r) = 2\rho U_\infty V_z(r,0). \tag{4.16}$$

Therefore in the linear limit, the load distribution on the disk is proportional to the axial velocity at the disk. However, there is no need to approximate (4.15) by (4.16) if we work directly with prescribed axial velocity at the actuator disk. In this case, the only approximation made by the theory is to neglect the contraction of the vortex tubes.

An arbitrary radial distribution of axial velocity can be split into a constant velocity distribution and a distribution which vanishes at the rim of the actuator disk. The resultant velocity fields are then the sums of the fields induced by these two distributions. Since we have already solved for the fields induced by a constant velocity distribution, without loss of generality we can assume that the load vanishes at the rim of the disk. Integrating (4.9) to (4.13) by parts and exploiting standard Bessel identities and the properties of Hankel transforms results in the alternative expressions below for any distribution which falls to zero at the actuator disk rim:

$$V_r(r,z) = -\int_0^{R_a}\int_0^\infty V_z(r',0)\mathrm{e}^{-s|z|}sr'J_0(sr')J_1(sr)\mathrm{d}s\,\mathrm{d}r', \tag{4.17}$$

$$V_z(r,z) = 2V_z(r,0) - \int_0^{R_a}\int_0^\infty V_z(r',0)\mathrm{e}^{-s|z|}sr'J_0(sr')J_0(sr)\mathrm{d}s\,\mathrm{d}r' \quad (z \geqslant 0), \tag{4.18}$$

$$V_z(r,z) = \int_0^{R_a}\int_0^\infty V_z(r',0)\mathrm{e}^{-s|z|}sr'J_0(sr')J_0(sr)\mathrm{d}s\,\mathrm{d}r' \quad (z < 0), \tag{4.19}$$

$$A_\phi(r,z) = \frac{2}{r}\int_0^r r'V_z(r',0)\mathrm{d}r' - \int_0^{R_a}\int_0^\infty V_z(r',0)\mathrm{e}^{-s|z|}r'J_0(sr')J_1(sr)\mathrm{d}s\,\mathrm{d}r' \quad (z \geqslant 0), \tag{4.20}$$

$$A_\phi(r,z) = \int_0^{R_a}\int_0^\infty V_z(r',0)\mathrm{e}^{-s|z|}r'J_0(sr')J_1(sr)\mathrm{d}s\,\mathrm{d}r' \quad (z < 0). \tag{4.21}$$

4.2. *Azimuthal velocity induced by the longitudinal vortex system*

The azimuthal velocity is zero outside the slipstream and does not vary with axial position within the slipstream. From Stokes's theorem, it is given by

$$V_\phi(r,z) = \frac{\Gamma_s(r)}{2\pi r}, \tag{4.22}$$

where $\Gamma_s(r)$ is the total axial flux of vorticity within radius r of the axis of symmetry. From vortex conservation, then $\Gamma_s(r)$ is also equal to the total strength of the lifting line vortices of the propeller blades at radius r.

4.3. *Circulation distribution*

From the Kutta–Joukowski law, the element of thrust dT acting on the propeller blades in the annular region between r and $r+dr$ for a propeller rotating with angular velocity Ω is given by

$$dT = \rho\left(\Omega r - \frac{V_\phi(r,\infty)}{2}\right)\Gamma_s(r)dr. \tag{4.23}$$

This can be integrated to give a total thrust

$$T = \rho\int_0^{R_a}\left(\Omega r' - \frac{V_\phi(r',\infty)}{2}\right)\Gamma_s(r')dr'. \tag{4.24}$$

Similarly, the total torque Q is given by

$$Q = \rho\int_0^{R_a} r'(U_\infty + V_z(r',0))\Gamma_s(r')dr'. \tag{4.25}$$

The thrust on an annular region of the actuator disk can also be calculated from the pressure discontinuity given by (4.15). This gives

$$dT = 2\pi\rho r\left(2V_z(r,0)(U_\infty + V_z(r,0)) - \frac{V_\phi^2(r,\infty)}{2}\right)dr. \tag{4.26}$$

Equating (4.23) and (4.26) and making use of (4.22), it is simple to show that the blade-bound circulation $\Gamma_s(r)$ is given by

$$\Gamma_s(r) = \frac{4\pi V_z(r,0)(U_\infty + V_z(r,0))}{\Omega}. \tag{4.27}$$

In the linear limit this gives

$$V_z(r,0) = \frac{\Omega\Gamma_s(r)}{4\pi U_\infty}. \tag{4.28}$$

4.4. *Optimum distributions*

Optimum circulation or axial velocity distributions for the actuator disk can be derived from the equations above using the calculus of variations. This can be done by minimizing the functional $F(\Gamma_s(r)) \equiv Q - lT$, where l is a constant Lagrange multiplier which is then chosen so as to give the correct thrust. Since in this case the functional F does not depend explicitly on $d\Gamma_s/dr$, then the Euler–Lagrange equation reduces to

$$\frac{\partial Q}{\partial\Gamma_s} = l\frac{\partial T}{\partial\Gamma_s}. \tag{4.29}$$

For contra-rotating propellers, $V_\phi(r,\infty)$ is zero and (4.29) gives the simple result that $V_z(r,0) = const$ is the optimum axial inflow distribution. For single-rotating propellers, making use of (4.14), the constant Lagrange multiplier can be shown to be

$$l = \frac{r(U_\infty + V_z(r,\infty))}{\Omega r - V_\phi(r,\infty)}, \tag{4.30}$$

and the optimum circulation distribution is given by

$$\Gamma_s(r) = \frac{2\pi(l\Omega - U_\infty)r^2}{l + \Omega r^2/U_\infty}. \tag{4.31}$$

More detailed derivations of (4.30) and (4.31) are given by Breslin & Andersen (1994). Equation (4.30) is the well-known condition of Betz (1919), which also holds approximately for the case of a finite number of blades. This condition means that in the ultimate wake of the propeller, the streamlines lie along true helicoidal surfaces. The potential jump across each helicoidal surface gives directly the bound circulation of the corresponding blade section and the helix angle β_{hel} at radius r is given by

$$\tan \beta_{hel} = l/r. \tag{4.32}$$

In the limit of a lightly loaded propeller, the perturbation velocities in the ultimate wake can be neglected and the tip helix angle is given by (4.30) and (4.32) as

$$\tan \beta_{tip} = J/\pi, \tag{4.33}$$

where $J \equiv U_\infty/nd$ is the propeller advance ratio, and d is the propeller diameter.

To this level of approximation, the helicoidal stream surfaces move downstream at the free-stream velocity. If we do not neglect the perturbation velocities, then (4.30) is used to define a constant artificial velocity, the displacement velocity w^*, through the relation

$$\frac{U_\infty + w^*}{\Omega} = l. \tag{4.34}$$

The helicoidal stream surfaces move downstream relative to the actuator disk at velocity $U_\infty + w^*$. If d' is the final contracted diameter of the slipstream, then the wake advance ratio J^* is defined as

$$J^* = \frac{U_\infty + w^*}{nd'}, \tag{4.35}$$

and

$$\tan \beta_{tip} = J^*/\pi. \tag{4.36}$$

The optimum distributions derived above are not very good approximations for the finite blade case, because they do not vanish at the rim of the actuator disk. Optimum distributions for lightly loaded single-rotating propellers with a finite number of blades were derived by Goldstein (1929) by solving for the flow in the ultimate wake using the Betz condition. Goldstein's distributions depend on the advance ratio J, and Theodorsen (1944) extended Goldstein's results to the heavily loaded propeller by using the wake advance ratio J^* rather than J. Hough & Ordway (1965) have suggested that for practical blade numbers and advance ratios, the Goldstein optimum distributions can be approximated by

$$\frac{\Gamma_s(r)}{U_\infty R_a} = A \frac{r}{R_a} \left(1 - \frac{r}{R_a}\right)^{1/2}. \tag{4.37}$$

Stern *et al.* (1988) have used this distribution in their Navier–Stokes calculations.

Theodorsen (1944) has used the Betz condition and the analogy between the flow of electric current and the flow of an ideal fluid to obtain optimum distributions for contra-rotating propellers with a finite number of blades from electrolytic tank measurements. He also verified that the Goldstein optimum distributions for single-rotating propellers could be directly measured in this manner. Theodorsen's optimum

No of blades	J^*	B
2+2	1.89	1.35
2+2	3.14	1.49
2+2	6.00	1.57
4+4	1.55	1.81
4+4	3.11	1.22
4+4	6.34	0.97
6+6	1.55	2.22
6+6	3.12	1.50
6+6	6.41	0.88

TABLE 2. Representation of Theodorsen's distributions

distributions for contra-rotating propellers can be closely approximated by a sum of elliptic and parabolic distributions of the form

$$\frac{\Gamma_s(r)}{\Gamma_s(0)} = B\left(1-\left(\frac{r}{R_a}\right)^2\right)^{1/2} + (1-B)\left(1-\left(\frac{r}{R_a}\right)^2\right). \tag{4.38}$$

The values of B which give the best least-squares fit to Theodorsen's distributions are given in table 2 and the comparisons of (4.38) with Theodorsen's measurements are shown in figure 4. Analytic solutions for both elliptic and parabolic distributions are given later.

Beginning with the work of Lerbs (1952), many workers have developed design methods based on lifting-line theory to obtain optimum circulation distributions for propellers with a finite hub diameter, and which can include the effect of the hull wake and other factors in the optimization. An account of these methods is given by Breslin & Andersen (1994). Modern propellers are optimized according to cavitation and vibration criteria in addition to optimum efficiency, with the result that a very wide range of practical propeller blade circulation distributions are to be found in the literature. Most distributions are designed to fall to zero at the hub radius, although circulation carryover to the hub may also occur.

5. Methods of solution and results

5.1. *Simplified formulae along the axis of symmetry*

Before considering the general case, it is interesting to consider the axial velocity induced along the axis of symmetry, for which simplified formulae can be derived. For this case both (4.10) and (4.11) can be integrated immediately with respect to s (Gradshteyn & Ryzhik 1980) to give

$$V_z(0,z) = -\int_0^{R_a+\epsilon} \frac{\mathrm{d}V_z(r,0)}{\mathrm{d}r}\left\{1+\frac{z}{(r^2+z^2)^{1/2}}\right\}\mathrm{d}r. \tag{5.1}$$

The radial integration above can be performed analytically for many radial distributions of inflow velocity. For example, for a constant distribution then

$$\frac{\mathrm{d}V_z(r,0)}{\mathrm{d}r} = -V_{z0}\delta(r-R_a),$$

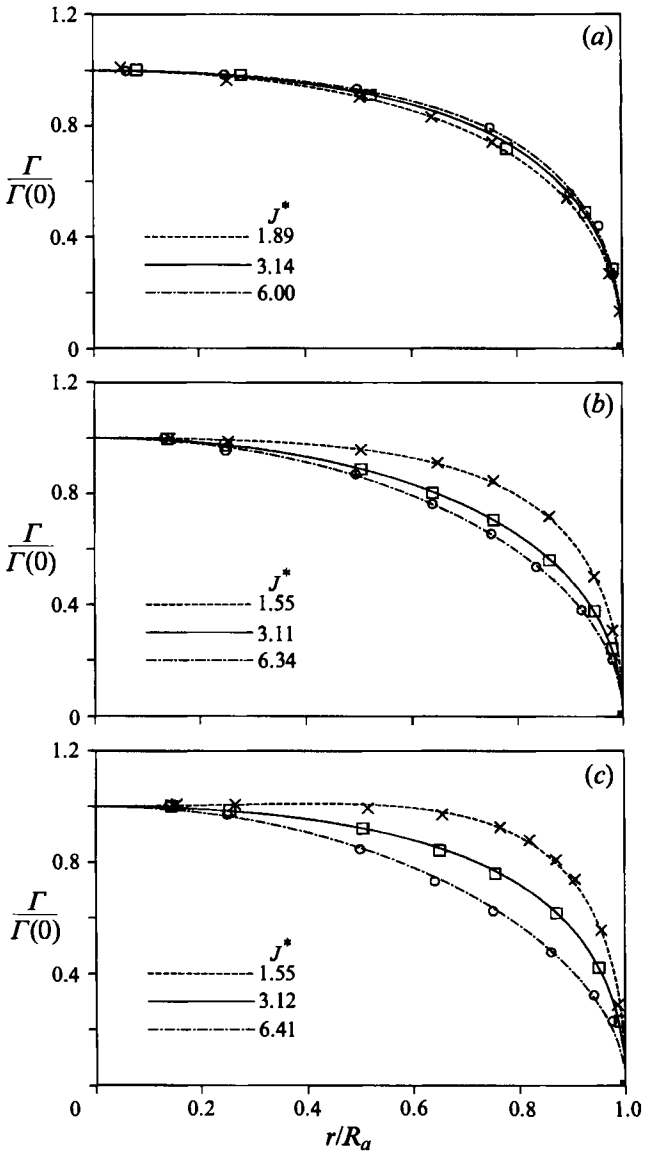

FIGURE 4. Theodorsen's optimum circulation distributions for contra-rotating propellers with varous wake advance ratios. (*a*) 2+2 blade contra-rotating propellers. (*b*) 4+4 blade contra-rotating propellers. (*c*) 6+6 blade contra-rotating propellers. The lines show equation 4.38 and the symbols show the results of Theodorsen's electrolytic tank measurements.

hence

$$V_z(0,z) = V_{z0}\left\{1 + \frac{z}{(R_a^2 + z^2)^{1/2}}\right\},$$

which recovers (3.8). Other results for distributions which vanish at $r = R_a$ are

$$V_z(0,z) = V_{z0}\left\{1 + \frac{z}{R_a}\left[\ln(R_a + (R_a^2 + z^2)^{1/2}) - \ln(|\,z\,|)\right]\right\} \text{ (linear)}, \qquad (5.2)$$

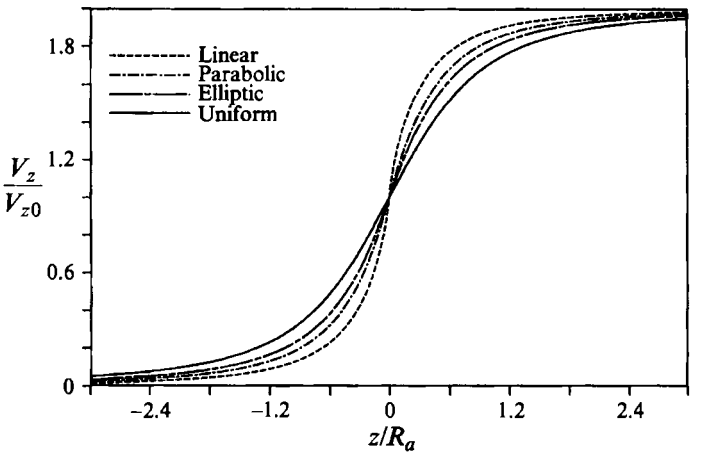

FIGURE 5. The variation of the axial velocity along the axis of symmetry for various radial load distributions.

$$V_z(0,z) = V_{z0}\left\{1 + \frac{2z}{R_a}\left[\left(1 + \left(\frac{z}{R_a}\right)^2\right)^{1/2} - \frac{|z|}{R_a}\right]\right\} \text{ (parabolic)}, \tag{5.3}$$

$$V_z(0,z) = V_{z0}\left\{1 + \frac{z}{2R_a}\left[\frac{\pi}{2} - \arcsin\left(\frac{z^2 - R_a^2}{z^2 + R_a^2}\right)\right]\right\} \text{ (elliptic)}. \tag{5.4}$$

The axial velocity distributions above are compared in figure 5. The downstream steady-state value is reached more rapidly for distributions which concentrate the load closer to the centre of the actuator disk.

5.2. *Analytic solutions for an even polynomial distribution*

The key to analytic solution of the generalized actuator disk equations derived earlier is the integral below, given by Gradshteyn & Ryzhik (1980), which is a variant of a well-known integral which Watson (1944) attributes to Sonine (1880):

$$\int_0^1 x^{\nu+1}(1-x^2)^{\mu} J_\nu(bx)\mathrm{d}x = 2^\mu \Gamma(\mu+1) b^{-(\mu+1)} J_{\nu+\mu+1}(b). \tag{5.5}$$

This integral allows the radial integration in (4.17) to (4.21) to be performed first for any radial distribution of axial velocity of the form

$$V_z(r,0) = V_{z0}\left\{1 - \left(\frac{r}{R_a}\right)^2\right\}^{\mu}. \tag{5.6}$$

The results of the integration are

$$V_r(r,z) = -\frac{2^\mu \Gamma(\mu+1) V_{z0}}{R_a^{\mu-1}} \int_0^\infty \frac{\mathrm{e}^{-s|z|} J_{\mu+1}(sR_a) J_1(sr)}{s^\mu}\mathrm{d}s, \tag{5.7}$$

$$V_z(r,z) = 2V_z(r,0) - \frac{2^\mu \Gamma(\mu+1) V_{z0}}{R_a^{\mu-1}} \int_0^\infty \frac{\mathrm{e}^{-s|z|} J_{\mu+1}(sR_a) J_0(sr)}{s^\mu}\mathrm{d}s \ (z \geqslant 0), \tag{5.8}$$

$$V_z(r,z) = \frac{2^\mu \Gamma(\mu+1) V_{z0}}{R_a^{\mu-1}} \int_0^\infty \frac{e^{-s|z|} J_{\mu+1}(sR_a) J_0(sr)}{s^\mu} ds \quad (z < 0), \tag{5.9}$$

$$A_\phi(r,z) = \frac{2}{r} \int_0^r r' V_z(r',0) dr' - \frac{2^\mu \Gamma(\mu+1) V_{z0}}{R_a^{\mu-1}} \int_0^\infty \frac{J_{\mu+1}(sR_a) J_1(sr)}{s^{\mu+1}} e^{-s|z|} ds \quad (z \geqslant 0), \tag{5.10}$$

$$A_\phi(r,z) = \frac{2^\mu \Gamma(\mu+1) V_{z0}}{R_a^{\mu-1}} \int_0^\infty \frac{J_{\mu+1}(sR_a) J_1(sr)}{s^{\mu+1}} e^{-s|z|} ds \quad (z < 0). \tag{5.11}$$

The remaining integrations with respect to s in (5.7) to (5.11) are all of the form

$$I_{(\lambda,\mu,\nu)} = \int_0^\infty s^\lambda J_\mu(sR_a) J_\nu(sr) e^{-s|z|} ds. \tag{5.12}$$

For λ, μ and ν integers, then integrals of the form defined by (5.12) can always be evaluated in terms of elliptic integrals using recursion relations derived from standard Bessel identities, as shown in the Appendix.† A number of the simpler integrals of this type are tabulated by Prudnikov *et al.* (1992), although sometimes with typographical errors.

By superposition of axial velocity distributions of the type described by (5.6), closed-form solutions can be obtained for the general distribution below, which can approximate any practical distribution with finite radial gradient to any desired accuracy for N sufficiently large:

$$V_z(r,0) = \sum_{n=0}^{N} a_n \left(\frac{r}{R_a}\right)^{2n}. \tag{5.13}$$

Wu (1962) has based his iterative method for the heavily loaded actuator disk on this distribution. A distribution with an infinite radial gradient at the blade tips cannot be adequately approximated by (5.13) alone, and it is necessary to include an additional basis function with the appropriate edge singularity. In the usual lifting-line theory of finite wings or propellers, the only typical spanwise distributions which have infinite tip gradients have square-root behaviour near the tips. A distribution of this type is the elliptic distribution and other distributions with square-root behaviour at the blade tips, such as (4.37), can be represented as the sum of an even polynomial distribution and an elliptic distribution, for which the solution is given later as a special case. The method of Lerbs (1952) predicts optimum circulation distributions for a propeller with finite hub which have an additional square-root singularity in the radial gradient at the hub radius. Solutions for a further basis function with this type of singularity are best obtained by integrating (4.17) to (4.21) first with repect to s, which gives a method similar to that of Hough & Ordway (1965). In practice, circulation carryover to the hub would prevent the build-up of infinite vortex density at the propeller-hub junction.

The solutions for distributions described by (5.13) become increasingly complex as n increases, but this is not a problem when solving using recursion on a computer, and a small FORTRAN program using the routines of Press *et al.* (1992) has been implemented to solve cases of this type. Here explicit formulae will only be given for the simplest case of parabolic loading.

† The Appendix is held in the editorial files and a copy may be obtained on request from the author or the Journal of Fluid Mechanics editorial office.

5.2.1. *Parabolic loading*

For parabolic loading the prescribed inflow velocity is

$$V_z(r,0) = \frac{V_{z0}}{R_a^2}(R_a^2 - r^2). \tag{5.14}$$

With k and β as defined earlier in (3.2), the radial velocity is given by

$$\begin{aligned} V_r(r,z) = &-\frac{V_{z0}}{\pi}\left(\frac{r}{R_a}\right)^{1/2}\left[\frac{4r}{R_a} - \frac{8(2-k^2)}{3k^2}\right]\frac{\mathrm{E}(k)}{k} \\ &-\frac{V_{z0}}{\pi}\left(\frac{r}{R_a}\right)^{1/2}\left[\frac{(4-k^2)(4-3k^2)}{3k^4} - \frac{r^2}{R_a^2}\right]k\mathrm{K}(k) \\ &-\frac{V_{z0}r}{R_a^2}(z\Lambda_0(\beta,k) - 2\mid z\mid)\ (r < R_a), \end{aligned} \tag{5.15}$$

$$\begin{aligned} V_r(r,z) = &-\frac{V_{z0}}{\pi}\left(\frac{r}{R_a}\right)^{1/2}\left[\frac{4r}{R_a} - \frac{8(2-k^2)}{3k^2}\right]\frac{\mathrm{E}(k)}{k} \\ &-\frac{V_{z0}}{\pi}\left(\frac{r}{R_a}\right)^{1/2}\left[\frac{(4-k^2)(4-3k^2)}{3k^4} - \frac{r^2}{R_a^2}\right]k\mathrm{K}(k) + \frac{V_{z0}r}{R_a^2}z\Lambda_0(\beta,k)\ (r > R_a). \end{aligned} \tag{5.16}$$

The radial velocity predicted by these equations is shown in figure 6 as a function of the radial coordinate for various axial locations. The radial field is a symmetric function of z and so only positive values of z are shown. The radial velocity component has its maximum well within the slipstream and has a continuous derivative at the vortical flow boundary. The maximum radial velocity at the disk is about 58% of the maximum induced axial velocity. In fact it is a feature of all of the solutions to be presented here that the induced radial velocity at the actuator disk is of the same order as the induced axial velocity, and therefore the assumption often made in developing actuator disk theory (for example Von Mises 1945) that the induced radial velocity can be neglected compared to the induced axial component is totally without foundation.

The axial velocity component for parabolic loading is given by

$$\begin{aligned} V_z(r,z) = &\frac{V_{z0}}{R_a^2}(R_a^2 - r^2 - 2z\mid z\mid) + \frac{6V_{z0}z}{\pi}\left(\frac{r}{R_a^3}\right)^{1/2}\frac{\mathrm{E}(k)}{k} \\ &+V_{z0}\left\{-\frac{zk(z^2+4r^2)\mathrm{K}(k)}{2\pi\,(rR_a^5)^{1/2}} + \left(\frac{\mid R_a^2 - r^2\mid +2z^2}{2R_a^2}\right)\Lambda_0(\beta,k)\right\}\ (r < R_a), \end{aligned} \tag{5.17}$$

$$\begin{aligned} V_z(r,z) = &\frac{6V_{z0}z}{\pi}\left(\frac{r}{R_a^3}\right)^{1/2}\frac{\mathrm{E}(k)}{k} \\ &+V_{z0}\left\{-\frac{zk(z^2+4r^2)\mathrm{K}(k)}{2\pi\,(rR_a^5)^{1/2}} + \left(\frac{\mid R_a^2 - r^2\mid -2z^2}{2R_a^2}\right)\Lambda_0(\beta,k)\right\}\ (r > R_a). \end{aligned} \tag{5.18}$$

The radial variation of axial velocity predicted by (5.17) and (5.18) at various axial locations is given in figure 7. Unlike the uniformly loaded disk, the axial velocity

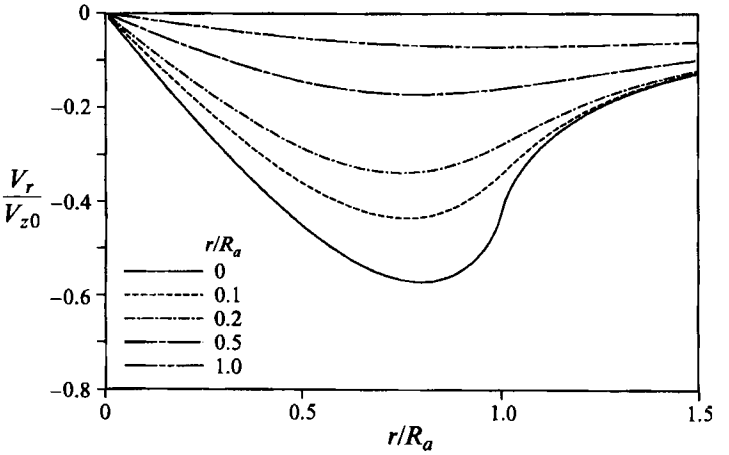

FIGURE 6. The radial variation of the radial velocity for parabolic loading. The radial velocity is a symmetric function of the axial coordinate.

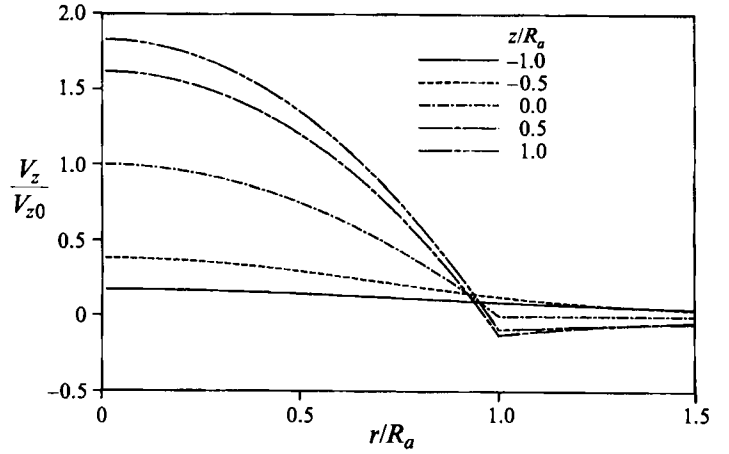

FIGURE 7. The radial variation of the axial velocity for parabolic loading.

is continuous across the vortical flow boundary, although the first derivative is discontinuous.

The vector potential for parabolic loading is

$$A_\phi(r,z) = \frac{V_{z0}z}{6\pi\,(rR_a^3)^{1/2}}\left(15r^2 - 3R_a^2 + \frac{4rR_a(k^2-2)}{k^2}\right)\frac{\mathrm{E}(k)}{k} + \frac{V_{z0}zk\mathrm{K}(k)}{24\pi\,(r^3R_a^5)^{1/2}}$$
$$\times\left(3\left[(R_a^2-r^2)z^2 - 6r^4 + 2R_a^2(r^2+R_a^2)\right] + 2r^2R_a^2\left[\frac{16-32k^2+19k^4-3k^6}{k^4(1-k^2)}\right]\right)$$
$$+V_{z0}\left(\frac{2r^2(\mid R_a^2-r^2\mid +2z^2) - \mid R_a^4-r^4\mid}{8rR_a^2}\right)\Lambda_0(\beta,k)$$
$$+\frac{V_{z0}r}{2}\left(1-\frac{r^2}{2R_a^2}-\frac{2z\mid z\mid}{R_a^2}\right)(r<R_a) \qquad (5.19)$$

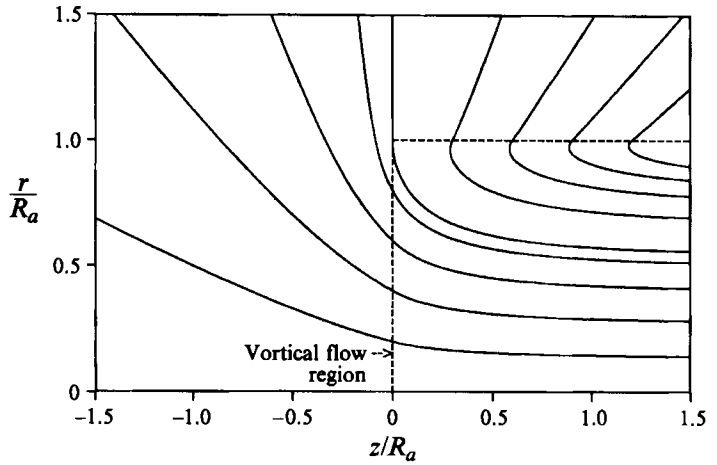

FIGURE 8. The perturbation streamline pattern for parabolic loading. The broken line encloses the region of non-zero vorticity.

and

$$A_\phi(r,z) = \frac{V_{z0}z}{6\pi\,(rR_a^3)^{1/2}}\left(15r^2 - 3R_a^2 + \frac{4rR_a(k^2-2)}{k^2}\right)\frac{\mathrm{E}(k)}{k} + \frac{V_{z0}zk\mathrm{K}(k)}{24\pi\,(r^3R_a^5)^{1/2}}$$
$$\times\left(3\left[(R_a^2-r^2)z^2 - 6r^4 + 2R_a^2(r^2+R_a^2)\right] + 2r^2R_a^2\left[\frac{16-32k^2+19k^4-3k^6}{k^4(1-k^2)}\right]\right)$$
$$+V_{z0}\left(\frac{2r^2(|\,R_a^2-r^2\,|-2z^2) - |\,R_a^4-r^4\,|}{8rR_a^2}\right)\Lambda_0(\beta,k) + \frac{V_{z0}R_a^2}{4r}\,(r>R_a). \quad (5.20)$$

The perturbation flow streamline pattern derived from (5.19) and (5.20) is plotted in figure 8.

5.3. *Solution with finite hub: P-1842 and P-1843 propellers*

The method is easily extended to handle a finite hub. If $H(r)$ is the Heaviside step function and R_h the hub radius then the axial inflow velocity for a finite hub can be written as

$$V_z(r,0) = H(R_a-r)\sum_{n=0}^{N} a_n\left(\frac{r}{R_a}\right)^{2n} - H(R_h-r)\sum_{n=0}^{N} b_n\left(\frac{r}{R_h}\right)^{2n} \quad (5.21)$$

where

$$b_n = a_n\left(\frac{R_h}{R_a}\right)^{2n}.$$

This reduces the finite hub case to a superposition of two hubless flows.

Circulation distributions are given by Johnsson (1983) for a series of five-bladed container-ship propellers with $R_h = 0.2R_a$ and these distributions have been reproduced in the recent book by Breslin & Andersen (1994). The circulation distribution for the P-1842 and P-1843 propellers can be represented for $R_h < r < R_a$ by an even polynomial with coefficients a_n given in table 3. The radial distributions of V_r and V_z induced by this circulation distribution at various axial positions are given in figures 9(*a*) and 9(*b*) respectively. The radial velocity reverses direction for

Coefficient	Numerical value
a_0	−0.37
a_1	15.79
a_2	−43.65
a_3	111.22
a_4	−165.82
a_5	126.36
a_6	−38.53

TABLE 3. Coefficients for Johnsson's distribution

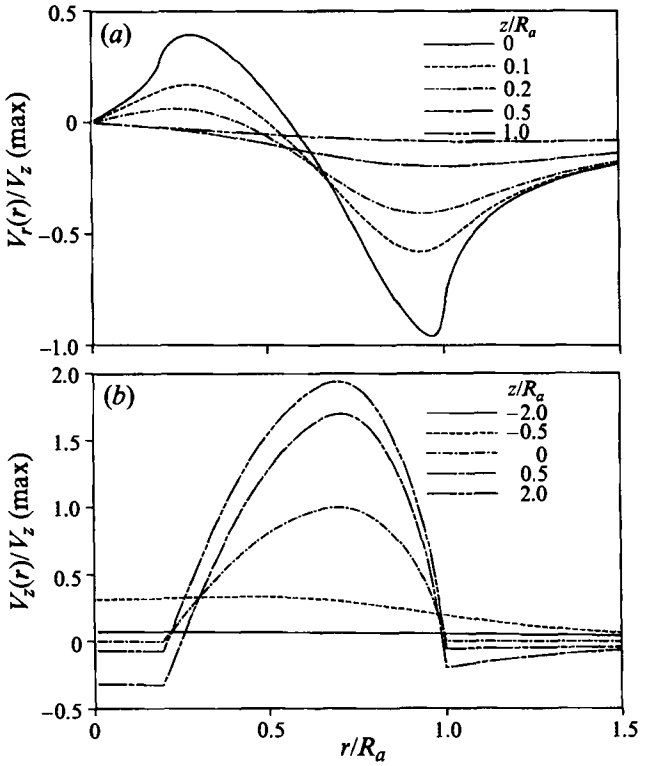

FIGURE 9. The radial variation of (*a*) radial velocity and (*b*) axial velocity for a five-blade container-ship propeller with a finite hub. The hub radius is 0.2 of the disk radius.

axial stations close to the actuator disk and has its maximum magnitude in the plane of the disk near the disk rim. The slope of the distribution is continuous at both the disk and hub radii. The axial flow is antisymmetric about the actuator disk plane for both $r < R_h$ and $r > R_a$. Figure 10 gives the corresponding perturbation streamline pattern. In addition to slipstream contraction at the outer boundary of the vortical flow region, the flow exhibits initial slipstream expansion at the inner boundary followed by final contraction to the hub radius at downstream infinity. The flow behind the actuator disk within the region enclosed by the streamline passing through the inner edge of the actuator disk at $r = R_h$ is recirculating, with the recirculation region centred within the vortical flow region.

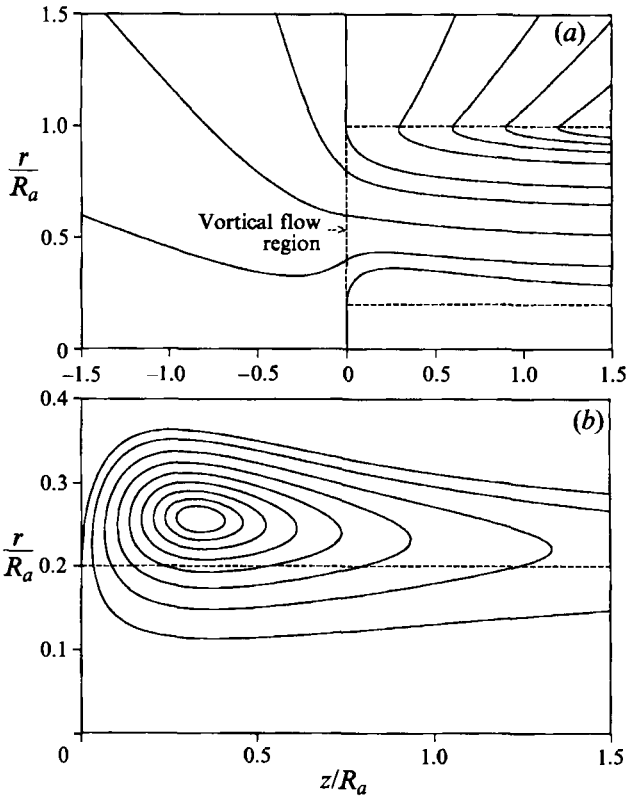

FIGURE 10. The perturbation streamline pattern for a five-blade container-ship propeller with a finite hub. The flow behind the actuator disk, within the innermost streamline passing through the disk, is recirculating. (*a*) Overall streamline pattern. (*b*) Streamlines in recirculating flow region.

5.4. *Solution for elliptic loading*

Elliptic loading is a special case for which the solution can be stated in terms of elementary functions. The inflow velocity is

$$V_z(r,0) = \frac{V_{z0}}{R_a}\left(R_a^2 - r^2\right)^{1/2}. \tag{5.22}$$

Therefore the radial integrations in (4.17) to (4.21) are equivalent to

$$I_r = V_{z0}R_a^2 \int_0^1 (1-t^2)^{1/2} t J_0(sR_a t)\mathrm{d}t. \tag{5.23}$$

Integrating using (5.5) gives

$$I_r = V_{z0}\left(\frac{\pi R_a}{2s^3}\right)^{1/2} J_{3/2}(sR_a). \tag{5.24}$$

The Bessel function in (5.24) can be expressed in terms of elementary functions (Gradshteyn & Ryzhik 1980) which gives

$$I_r = \frac{-V_{z0}}{sR_a}\frac{\mathrm{d}}{\mathrm{d}s}\left(\frac{\sin(sR_a)}{s}\right). \tag{5.25}$$

Substituting (5.25) into (4.17) to (4.18), integrating by parts and using standard Bessel integrals (Gradshteyn & Ryzhik 1980) gives

$$V_r(r,z) = \frac{V_{z0}\,|\,z\,|}{2r}\left(\frac{1}{\alpha}-\alpha\right) - \frac{V_{z0}r}{2R_a}\arcsin\left\{\frac{2R_a}{\left(z^2+(R_a+r)^2\right)^{1/2}+\left(z^2+(R_a-r)^2\right)^{1/2}}\right\}, \tag{5.26}$$

$$V_z(r,z) = 2V_z(r,0) + V_{z0}\left(-\alpha+\frac{z}{R_a}\arcsin\left\{\frac{2R_a}{\left(z^2+(R_a+r)^2\right)^{1/2}+\left(z^2+(R_a-r)^2\right)^{1/2}}\right\}\right) \quad (z \geqslant 0) \tag{5.27}$$

and

$$V_z(r,z) = V_{z0}\left(\alpha+\frac{z}{R_a}\arcsin\left\{\frac{2R_a}{\left(z^2+(R_a+r)^2\right)^{1/2}+\left(z^2+(R_a-r)^2\right)^{1/2}}\right\}\right) \quad (z<0). \tag{5.28}$$

$$A_\phi(r,z) = \frac{2V_{z0}R_a^2}{3r}\left(1-\left[1-\left(\frac{r}{R_a}\right)^2\right]^{3/2}\right) - I_\phi(r,z) \quad (z \geqslant 0 \text{ and } r<R_a), \tag{5.29}$$

$$A_\phi(r,z) = \frac{2V_{z0}R_a^2}{3r} - I_\phi(r,z) \quad (z \geqslant 0 \text{ and } r>R_a), \tag{5.30}$$

$$A_\phi(r,z) = I_\phi(r,z) \quad (z<0). \tag{5.31}$$

where

$$I_\phi(r,z) = \frac{V_{z0}r\,|\,z\,|}{2R_a}\arcsin\left\{\frac{2R_a}{\left(z^2+(R_a+r)^2\right)^{1/2}+\left(z^2+(R_a-r)^2\right)^{1/2}}\right\} + \frac{V_{z0}r}{4}\left(\frac{z^2}{r^2}\frac{(1+\alpha)(1-\alpha)^2}{\alpha^2} - \frac{R_a^2(1-\alpha)^3}{3r^2} - (1+\alpha)\right). \tag{5.32}$$

In the equations above α is a dimensionless parameter given by

$$\alpha = \left(\frac{\left((R_a^2-r^2-z^2)^2+4R_a^2z^2\right)^{1/2}+R_a^2-r^2-z^2}{2R_a^2}\right)^{1/2}. \tag{5.33}$$

In the plane of the actuator disk, the radial velocity field reduces to the simple equations below:

$$V_r(r,0) = -\frac{V_{z0}\pi r}{4R_a} \quad (r \leqslant R_a), \tag{5.34}$$

$$V_r(r,0) = \frac{V_{z0}}{2}\left\{\left(1-\frac{R_a^2}{r^2}\right)^{1/2} - \frac{r}{R_a}\arcsin\left(\frac{R_a}{r}\right)\right\} \quad (r>R_a). \tag{5.35}$$

Hence an elliptic axial velocity inflow at the actuator disk corresponds to a linear radial velocity inflow at the disk. The maximum magnitude of the radial velocity is $\frac{1}{4}\pi V_{z0}$, which occurs at the disk rim. The radial distribution of V_r given by (5.26) is

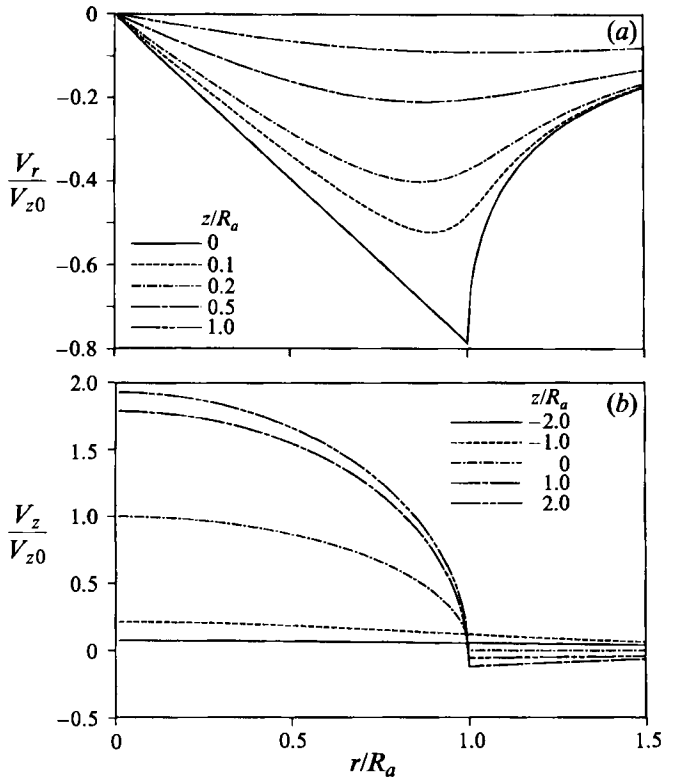

FIGURE 11. The radial variation of (*a*) the radial velocity and (*b*) the axial velocity for the elliptically loaded actuator disk.

shown for various axial locations in figure 11(*a*). The radial distribution of V_z is given for various axial positions in figure 11(*b*). The perturbation flow streamline pattern derived from (5.29) to (5.31) is shown in figure 12.

5.5. *Solution for a general polynomial loading*

If the radial integration of the general equations is performed last, then integral representations for velocities and vector potential can be obtained in terms of elementary functions. These integral representations may or may not be completely decomposable into elliptic integrals, as in the even polynomial case, but can always be evaluated numerically. Owing to the recursive nature of the solution, implementation of the method on a computer is simple.

5.5.1. *Radial velocity field*

Let

$$V_z(r,0) = \sum_{n=0}^{N} a_n r^n \tag{5.36}$$

and it is assumed that $V_z(R_a,0) = 0$. Equation (4.9) for the radial velocity component can be integrated with respect to s to give

$$V_r(r,z) = \frac{1}{\pi}\int_0^{R_a} \frac{\mathrm{d}V_z(r',0)}{dr'}\left(\frac{r'}{r}\right)^{1/2} Q_{1/2}\left(\frac{r'^2+r^2+z^2}{2rr'}\right)\mathrm{d}r'. \tag{5.37}$$

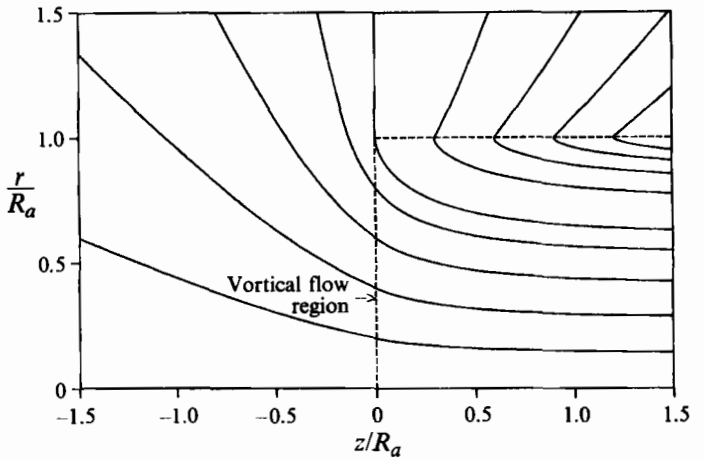

FIGURE 12. The perturbation streamline pattern for the elliptically loaded actuator disk.

Substituting (5.36) into (5.37) and replacing $Q_{1/2}$ by its integral representation gives

$$V_r(r,z) = \frac{1}{\pi}\sum_{n=1}^{N} \int_0^{R_a}\int_0^{\pi} \frac{na_n r'^n \cos(t)\mathrm{d}t\,\mathrm{d}r'}{(r'^2 + r^2 + z^2 - 2r'r\cos t)^{1/2}}. \tag{5.38}$$

Reversing the order of integration, the r' integration can be performed for all values of n using recursion. Let $X(r',t,r,z) = r'^2 + r^2 + z^2 - 2r'r\cos t$, and let

$$I_n(r',t,r,z) \equiv \int \frac{r'^n \mathrm{d}r'}{(X(r',t,r,z))^{1/2}}. \tag{5.39}$$

Then $I_n(r',t,r,z)$ can be calculated from the recursion relation below (Gradshteyn & Ryzhik 1980):

$$I_n(r',t,r,z) = \frac{r'^{n-1}}{n}\left(X(r',t,r,z)\right)^{1/2} + \frac{(2n-1)r\cos t}{n} I_{n-1}(r',t,r,z) - \frac{n-1}{n} I_{n-2}(r',t,r,z). \tag{5.40}$$

The starting integrals for the recursion are

$$I_0(r',t,r,z) = \ln\left[2\left(X(r',t,r,z)\right)^{1/2} + 2(r' - r\cos t)\right], \tag{5.41}$$

$$I_1(r',t,r,z) = \left(X(r',t,r,z)\right)^{1/2} + r\cos t I_0(r',t,r,z). \tag{5.42}$$

Hence the radial velocity field is given by

$$V_r(r,z) = \frac{1}{\pi}\int_0^{\pi} \cos t \left\{\sum_{n=1}^{N} na_n(I_n(R_a,t,r,z) - I_n(0,t,r,z))\right\} \mathrm{d}t. \tag{5.43}$$

5.5.2. *Axial velocity field*

Solution of the axial velocity field using (4.18) and (4.19) is equivalent to evaluation of the integral

$$I(r,z) = \mp\frac{\partial}{\partial z}\int_0^{R}\int_0^{\infty} \mathrm{e}^{-s|z|} V_z(r',0) r' J_0(sr') J_0(sr)\mathrm{d}s\,\mathrm{d}r'. \tag{5.44}$$

Performing the s-integration gives

$$I(r,z) = \mp\frac{1}{\pi}\frac{\partial}{\partial z}\int_0^{R_a} V_z(r',0)\left(\frac{r'}{r}\right)^{1/2} Q_{-1/2}\left\{\frac{r'^2+r^2+z^2}{2rr'}\right\}\mathrm{d}r'. \tag{5.45}$$

Proceeding as for the radial velocity component, and performing the differentiation with respect to z gives

$$I(r,z) = \frac{|z|}{\pi}\int_0^{\pi}\mathrm{d}t\sum_{n=0}^{N} a_n\int_0^{R_a}\frac{r'^{n+1}\mathrm{d}r'}{(r'^2+r^2+z^2-2rr'\cos t)^{3/2}}. \tag{5.46}$$

As before, the radial integration in (5.46) can be performed for all values of n by recursion. Let

$$\hat{I}_n(r',t,r,z) = \int\frac{r'^{n+1}\mathrm{d}r'}{X(r',t,r,z)^{3/2}}. \tag{5.47}$$

Then the recursion relation for the $\hat{I}_n$ is (Gradshteyn & Ryzhik 1980)

$$\hat{I}_n(r',t,r,z) = \frac{r'^n}{(n-1)(X(r',t,r,z))^{1/2}} + \frac{(2n-1)r\cos t}{n-1}\hat{I}_{n-1}(r',t,r,z) - \frac{n}{(n-1)}\hat{I}_{n-2}(r',t,r,z). \tag{5.48}$$

The starting integrals for this recursion are

$$\hat{I}_0(r',t,r,z) = -\frac{1-rr'\cos t}{(r^2\sin^2 t+z^2)(X(r',t,r,z))^{1/2}}, \tag{5.49}$$

$$\hat{I}_1(r',t,r,z) = -\frac{(z^2-r^2\cos 2t)r'+r\cos t}{(r^2\sin^2 t+z^2)(X(r',t,r,z))^{1/2}} + \ln\left[2\left(X(r',t,r,z)\right)^{1/2}+2(r'-r\cos t)\right]. \tag{5.50}$$

Hence the integral $I(r,z)$ is given by

$$I(r,z) = \frac{|z|}{\pi}\int_0^{\pi}\left\{\sum_{n=0}^{N} a_n(\hat{I}_n(R_a,t,r,z)-\hat{I}_n(0,t,r,z))\right\}\mathrm{d}t \tag{5.51}$$

and the solution for the axial velocity is

$$V_z(r,z) = 2V_z(r,z) - I(r,z)\ \ (z\geqslant 0), \tag{5.52}$$

$$V_z(r,z) = I(r,z)\ \ (z<0). \tag{5.53}$$

5.5.3. *Vector potential and stream function*

The vector potential is given by

$$A_\phi(r,z) = A_{\phi 1}(r) - A_{\phi 2}(r,z)\ \ (z\geqslant 0), \tag{5.54}$$

$$A_\phi(r,z) = A_{\phi 2}(r,z)\ \ (z<0), \tag{5.55}$$

where

$$A_{\phi 1}(r) = 2\sum_{n=0}^{N}\frac{a_n}{n+2}r^{n+1} \tag{5.56}$$

and

$$A_{\phi 2}(r,z) = \int_0^{R_a} \int_0^{\infty} \sum_{n=0}^{N} a_n r'^n e^{-s|z|} J_0(sr') J_1(sr) \mathrm{d}s \, \mathrm{d}r'. \tag{5.57}$$

Performing the s-integration in (5.57) and then substituting the integral representation given in the Appendix for the integral $I_{(0,0,1)}$ gives

$$A_{\phi 2}(r,z) = \sum_{n=0}^{N} \frac{a_n \mid z \mid}{\pi} \int_0^{R_a} \int_0^{\pi} \frac{\cos t}{r^2 \sin^2 t + z^2} \frac{r'^{n+1} \mathrm{d}t \, \mathrm{d}r'}{\left(r^2 + r'^2 + z^2 - 2rr' \cos t\right)^{1/2}}. \tag{5.58}$$

The radial integration in (5.58) above can be performed for all values of n to give

$$A_{\phi 2}(r,z) = \frac{\mid z \mid}{\pi} \int_0^{\pi} \left\{ \frac{r \cos^2 t}{r^2 \sin^2 t + z^2} \sum_{n=0}^{N} a_n (I_{n+1}(R_a,t,r,z) - I_{n+1}(0,t,r,z)) \right\} \mathrm{d}t$$
$$- \frac{\mid z \mid}{\pi} \int_0^{\pi} \left\{ \frac{\cos t}{r^2 \sin^2 t + z^2} \sum_{n=0}^{N} a_n (I_{n+2}(R_a,t,r,z) - I_{n+2}(0,t,r,z)) \right\} \mathrm{d}t. \tag{5.59}$$

In (5.59), the I_n are as defined above for the radial field case and satisfy the same recurrence relation. A small FORTRAN computer program has been written implementing the arbitrary polynomial method given above. This program has been checked against the closed-form solutions derived using the alternative method for even polynomials and was found to agree perfectly.

6. Comments and conclusions

A general method of solving analytically for the flow induced by a propeller actuator disk with an essentially arbitrary radial distribution of load has been developed. The method has been used to complete the solution of Hough & Ordway (1965) for the uniformly loaded actuator disk and was then applied to various radial distributions of load. The method shows that the induced radial velocity component in the plane of the actuator disk is comparable in magnitude with the induced axial component. It has been found that the optimum load distributions for a contra-rotating propeller with a finite number of blades obtained by Theodorsen (1944) from electrolytic tank measurements can be represented as a superposition of parabolic and elliptic distributions, which are the distributions which give the simplest explicit formulae. The method has been applied to a practical propeller case with a finite hub, and it was found that in the hub region there is slipstream expansion followed by contraction to the hub radius far downstream. The method is suitable for calculation of the slipstream effect on complex configurations by embedding it in a suitable boundary-integral method, and can be extended into the compressible flow regime using compressibility corrections.

The method applied here to the actuator disk will also solve all the analogous electromagnetic problems associated with both semi-infinite and finite solenoids and radial distributions of solenoids. The magnetic fields induced by a semi-infinite solenoid distribution are exactly analogous to the slipstream solutions presented here, and the fields induced by a radial distribution of solenoids of finite length is obtained by superposition of two semi-infinite distributions of opposite sign and axial relative displacement equal to the solenoid length.

The author would like to thank Dr Christopher Grigson and Dr Lars Soland for reading the manuscript and for their encouragement during the course of the work. Thanks are also due to the referees for their helpful suggestions.

REFERENCES

ABRAMOWITZ, M. & STEGUN I. S. 1972 *Handbook of Mathematical Functions.* Dover.

BASSET, A. B. 1888 *A Treatise on Hydrodynamics*, Vol. II. Deighton Bell.

BETZ, A. 1919 Schraubenpropeller mit geringstem Energieverlust. *Göttinger Nachr.*, pp. 193–217

BRESLIN, J. P. & ANDERSEN, P. 1994 *Hydrodynamics of Ship Propellers.* Cambridge University Press.

BYRD, P. F. & FRIEDMAN, M. D. 1971 *Handbook of Elliptic Integrals for Engineers and Scientists*, 2nd Edn. Springer.

CLARK, R. J. & VALAREZO, W. O. 1990 *AIAA*-90-0031, *28th Aerospace Sciences Meeting, Reno, Nevada.*

GRADSHTEYN, I. S. & RYZHIK, I. M. 1980 *Table of Integrals, Series, and Products.* Academic Press.

GREENBERG, M. D. & POWERS, S. R. 1970 *NASA Rep.* CR-1672.

GOLDSTEIN, S. 1929 *Proc. R. Soc. Lond.* A **123**, 440–465.

HOBSON, E. W. 1896 *Phil. Trans. R. Soc. Lond.* A **187**, 522.

HOUGH, G. R. & ORDWAY, D. E. 1965 *Developments in Theoretical and Applied Mechanics*, Vol. 2, pp. 317–336. Pergamon.

JOHNSSON, C. A. 1983 Propellers with reduced tip loading and unconventional blade form and blade sections. *Eighth School Lecture Series, Ship Design for Fuel Economy, WEGEMT, Göteborg.*

KONING, C. 1935 *Aerodynamic Theory*, Vol. 4 (ed. W.F. Durand). Guggenheim Fund for the Promotion of Aeronautics.

LAMB, H. 1932 *Hydrodynamics.* Cambridge University Press.

LERBS, H. W. 1952 *Soc. Naval Archit. Marine Engrs* **60**, 73–123.

PRESS, W. H., TEUKOLSKY, S. A., VETTERLING, W. T. & FLANNERY, B. P. 1992 *Numerical Recipes in FORTRAN.* Cambridge University Press.

PRUDNIKOV, A. P., BRYCHKOV, Y. A. & MARICHEV, O. I. 1992 *Integrals and Series, Vol. 4: Direct Laplace Transforms.* Gordon & Breach.

SONINE, N. J. 1880 *Math. Ann.* **16**, 1-80.

SPIEGEL, M. R. 1965 *Theory and Problems of Laplace Transforms.* Schaum.

STERN, F., KIM, H. T., PATEL, V. C. & CHEN, H. C. 1988 *J. Ship Res.* **32**, 246–262.

STRASH, D. J., NATHMAN, J. K., MASKEW, B. & DVORAK, F. A. 1984 *AIAA*-84-2178, *AIAA 2nd Applied Aerodynamics Conference, Seattle.*

THEODORSEN, T. 1944 *NACA Rep.* 775.

VON MISES, R. 1945 *Theory of Flight.* McGraw-Hill.

WATSON, G. N. 1944 *A Treatise on the Theory of Bessel Functions.* Cambridge University Press.

WU, T. Y. 1962 *Schiffstechnik.* **9**, No. 47, 134–138.